Composites Communications 25 (2021) 100730

Contents lists available at ScienceDirect

Composites Communications

journal homepage: www.elsevier.com/locate/coco

High hydrophobic poly(lactic acid) foams impregnating one-step Si–F modified lignin nanoparticles for oil/organic solvents absorption

Hui Ding [a], Weijun Yang [a,*], Wenhao Yu [a], Tianxi Liu [a], Haigang Wang [b], Pengwu Xu [a], Liangliang Lin [a], Piming Ma [a,**]

[a] The Key Laboratory of Synthetic and Biological Colloids, Ministry of Education, Jiangnan University, Wuxi, China
[b] Northeast Forestry University, Key Laboratory of Bio-based Material Science & Technology, Ministry of Education, Harbin, China

ARTICLE INFO

Keywords:
poly(lactic acid)
Lignin nanoparticles
Foams
Hydrophobicity
Oil/organic solvents absorption

ABSTRACT

In this work, the hydrophobic lignin nanoparticles (LNP) were synthesized by a synchronous modification of silanization and fluorination process. Thermogravimetric analyser, fourier-transform-infrared-spectroscopy, X-ray photoelectron spectroscopy and transmission electron microscopy were used to confirm the surface modified LNP (*m*-LNP). The maximum degradation temperature of *m*-LNP was 85 °C higher than that of origin LNP. Then the bio-based PLA foams were prepared via freezing-dry method by impregnating various amount of *m*-LNP. The results showed that a high hydrophobicity (141° of contact angle) and porosity structure (94% of porosity) were constructed when the *m*-LNP content increased to 6 wt% (PLA-6L). Afterwards, the absorption capacities of the PLA composite foams towards various oil/organic solvents are measured. The composite foams reached their saturated adsorption capacity in quite short time and exhibited good recyclability due to the two factors: high hydrophobicity and high porosity. Thus, the bio-based PLA/m-LNP composite foams could be used as the eco-benign and efficient absorbents for petroleum leakage, oil spills and toxic organic solvents in water contamination field.

1. Introduction

Water contamination arising from petroleum leakage, oil spills and toxic organic solvents discharge has become a strong global concern. In response, many porous materials have been developed as absorbents including inorganic nanowire membranes [1,2], activated carbon [3], zeolites [4], carbon nanotubes [5], graphene [6], organic polyurethane foam [7] and olefin resin [8]. However, most of the existing absorbent materials still maintained some ineluctable drawbacks such as high-cost, complicated fabrication procedures and difficulty of discarding etc. More importantly, the absorbents are generally chemically stable and non-biodegradable, which may cause new environment problem if mishandling. There is therefore a high demand for producing eco-friendly, low-cost and high absorption capacity sorbents from biopolymers.

Using the biodegradable biomass to produce absorbents with higher oil sorption capacity is one of the wise ways [9]. These biomass materials include cellulose [10] and chitosan/chitin [11]. As the second most abundant biopolymer, lignin has also been considered as a promising absorbent material for the oil/organic solvents removal, ascribing to its 3D aromatic structure consisting of hydrophobic phenyl propane skeleton and oxygen-contained branches. For example, Wang et al. [12] prepared lignin based xerogel by a sol–gel process and ambient pressure drying method after dissocyanate modification. Interestingly, the lignin xerogel not only presented excellent self-cleaning and super hydrophobicity ability, but also possessed high potential applications capacity as absorbent materials. Based on these finding, they subsequently developed a high-hydrophobic, ultralight and super oleophilic sponges based on lignin-melamine sponges, which consisted of an interconnected network with high porosity and low density (6.4 mg cm^{-3}). The results demonstrated that these sponges are quite suitable for applications in oil–water separation, as the sponge skeleton has a hydrophobic carbon coating surface. Consequently, this sponge showed excellent oil absorption behavior such as good recyclability and oil absorption capacity up to 99 v% of its own volume [13]. In the cases of polymer impregnated with lignin as the absorbents, Yoshida et al. [8] studied the influence of

* Corresponding author.
** Corresponding author.
E-mail addresses: weijun.yang@jiangnan.edu.cn (W. Yang), p.ma@jiangnan.edu.cn (P. Ma).

https://doi.org/10.1016/j.coco.2021.100730
Received 1 February 2021; Received in revised form 15 March 2021; Accepted 16 March 2021
Available online 28 April 2021

lignin concentration, which acted as the functional filler, on the crude oil sorption capacity in polyurethane foam (PUF). Although the incorporation of lignin showed decreased effects on the thermal stability and less hydrophobicity for the polyurethane foam, all the composite foams showed an enhancement in the oil absorption capacity, and the PUF with 10 wt% exhibited an improvement in capacity around 35.5% in comparison with PUF sample. Similarly, Chen et al. [6] also fabricated a compressive and fire-resistant graphene aerogel incorporated with various amount of lignin, which can be used for different toxic organic solvents. While increasing the lignin loading equal to graphene, the absorption capacity was improved significantly more than 200 times, which was much higher than that of pure graphene aerogel (91 times). They proposed that the addition of lignin would contribute better distribution of porous structure of the aerogels, making it more favorable in absorption for oil/organic solvents. However, most of these cases seldom investigate the effects of lignin modification on the absorption capacity.

In summary, high hydrophobic and well-distributed porous structure would contribute to enhancing the absorption capacity for the absorbent. Inspired from the former works, we therefore proposed the impregnation of lignin nanoparticles into the bio-degradable polymer, which is considered to be a promising and eco-friendly approach to efficiently absorb oil/organic solvents. In this work, we are attempting to construct the bio-based poly (lactic acid) PLA foam with high hydrophobicity and well-distributed porous structure, via a green and facile modification of lignin nanoparticles combined with freezing-dry method. Afterwards, the absorption capacities of various oil/organic solvents are measured. The effects of both modified lignin and foam structure on the absorption capacity will be well discussed. This work may pay the way to develop a fully biodegradable absorbent for the oil/organic contaminant.

2. Experimental section

2.1. Materials

Poly (lactic acid) (PLA 3001D, M_w = 150,000 Da, density = 1.24 g/cm^3) was supplied from Natureworks, USA. Lignin nanoparticles (LNP) were prepared referring our previous work [14]. 1H,1H,2H, 2H-perfluorooctyltriethoxysilane (FS, 98%), 3-(2-Aminoethylamino) -propyltrimethoxysilane (AS, 98%) and all the chemicals/organic solvents were purchased from Sinopharm Chemical Reagent Co., Ltd.

2.2. Modification of LNP and preparation of PLA hybrid foams

Modification of LNP was carried out through a wet chemical process in a deionized water solution where 1 wt% concentration of well-dispersed LNP was vigorously mixed with two different functional silanes, FS (0.6 v/v%) and AS (0.9 v/v%) for 8 h at room temperature, according to Ref. [15]. Before use, the modified LNP (*m*-LNP) was solvent exchanged to 1, 4-dioxane (1 wt%) by an extraction filtration process.

PLA foams impregnating with *m*-LNP was prepared according to the following procedures (Scheme 1). Firstly, 2.0 g of PLA was diluted in 1, 4-dioxane, and then various amount of *m*-LNP was added into the PLA solution to form well-dispersed mixture. Afterwards, the mixture solution was frozen at −20 °C in the refrigerator for overnight. Finally, the PLA hybrid foams with different amount of *m*-LNP were obtained by a freezing dry process [16]. It should be noted that the 1, 4-dioxane solvent could be recycled.

2.3. Characterizations of m-LNP and PLA foams

The thermal stability of *m*-LNP was investigated through a thermogravimetric analyser (TGA, Q500 TA instrument). The specimen around 5 mg was heated from 30 to 800 °C at 20 °C/min under N_2. The chemical states of *m*-LNP were examined using fourier transform infrared spectroscopy (FTIR, Nicolet 6700) with a resolution of 4 cm^{-1} using an attenuated total reflection (ATR) method. X-ray photoelectron spectroscopy (XPS) instrument (Shimadzu/Kratos, Ltd., Japan) equipped with a Mg Kα X-ray source was operated at 150 W. The morphology of LNP and *m*-LNP was also implemented by means of transmission electron microscopy (TEM, JEM-2100plus) [17].

The density of PLA hybrid foams was calculated by a mass/volume ratio method. The wettability of the foams was evaluated by water contact angle (WCA) via the Contact angle instrument (FTA 1000, USA) under static condition. The porous morphology of the PLA hybrid foams was observed via a Hitachi S-4800 Scanning Electron Microscope (SEM).

For the oil/organic solvent absorption measurements, Sudan Red 4/toluene mixture was used to simulate the leaked oil, then one piece of foam sample (same weight) was put into a 25 mL beaker containing 2 mL Sudan Red 4/toluene mixture on water surface and allowed to absorb at room temperature, the absorption time was recorded. The absorption for various organic solvents (*n*-hexane, toluene, waste peanut oil, ethyl acetate and conductive oil) were measured by immersed the foam samples into the solvent for 10 s, and then the absorption capacity of the sample was calculated with the following equation: Weight gain (Q) = $(W_t - W_0)/W_0 \times 100\%$, where W_0 and W_t are the sample weight before and after absorption, respectively. Alternatively, the absorption cycles were also measured using toluene as the absorbate and 5 cycles were tested.

3. Results and discussion

3.1. Characterizations of m-LNP

The variation in FTIR spectral features between unmodified and modified LNP is depicted in Fig. 1. The characteristic peaks between 1150 and 1000 cm^{-1} in the *m*-LNP are corresponding to the various stretching modes of Si–O–C and Si–O–Si vibration. Meanwhile, the variation at these characteristic peaks could also be responsible to the various stretching modes of –CF_2 and –CF_3 such as 1121, 1145 cm^{-1} in the modified LNP [15]. In the carbonyl/carboxyl region, the band at 1705–1720 cm^{-1}, originating from conjugated carbonyl-carboxyl stretching, disappeared and its shoulder bands 1660 cm^{-1} intensified that can be associated with the unconjugated carbonyl/carboxyl

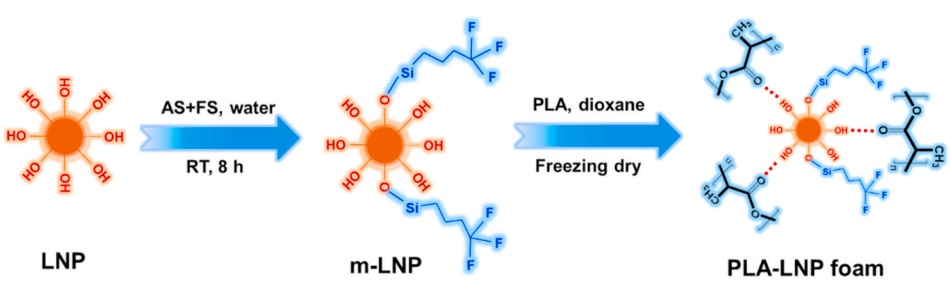

Scheme 1. The preparation process of PLA composite foams.

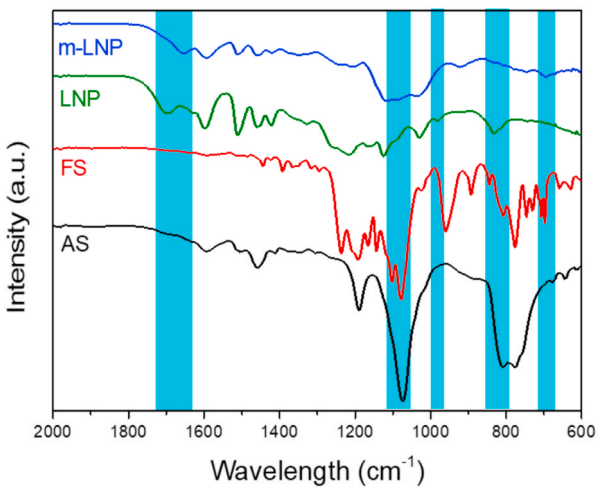

Fig. 1. The full FTIR spectra of AS, FS, LNP and *m*-LNP.

stretching [18]. Namely the unconjugated carbonyl/carboxyl stretching of carbonyl/carboxyl was enhanced, while the conjugated carbonyl/carboxyl stretching was weakened. The band at 830 cm^{-1}, which was associated with the C–H out-of-plane vibrations in position 2, 5 and 6 of *Guaiacyl* units, also changed. Lignin is an amphipathic polymer consisting of both hydrophilic groups (–OH and –COOH) and hydrophobic skeleton (aromatic moieties) [14,19]. Therefore, these results imply the variation in its chemical signature, which highlighted lowing the surface energy of LNP, turning to more hydrophobic structure [20].

Fig. 2a showed the XPS spectra of *m*-LNP. Compared with LNP (see SI), the new emerging F and Si demonstrated the successful modification of LNP. The fitting data of core level of C 1s, O 1s, N 1s, F 1s and Si 2s spectra peak area regions for the *m*-LNP spectra are available in Fig. S1. The chemical bonds of the fluorine groups were examined in detail from the high-resolution carbon C 1s. Three different lignin carbons (C–C/C–O/O–C═O) as well as two fluorine atoms at 292 and 294 eV (−CF_2 and –CF_3) could be observed in *m*-LNP sample [15,21]. The thermal stability of LNP and *m*-LNP were investigated by TGA and the results are presented in Fig. 2b. The maximum degradation temperature of *m*-LNP was registered at 455 °C, while the LNP was only 370 °C, i.e. an 85 °C enhancement was recorded. Meanwhile, the weight residue at 800 °C of *m*-LNP was 42.5 wt%, which was 4.3 wt% higher than that of LNP. The higher pyrolysis temperature for the *m*-LNP can be ascribed to the introduction of Si–O bonds, which will enhance the lignin skeleton stability due to the formation of Si–O–C networks [22]. These results indicated that the silanization modification combined with fluorination of LNP was beneficial to prominently improve the thermal behavior of lignin. Fig. 2c and d showed the morphology of the LNP and *m*-LNP. The lignin nanoparticles elucidate a typical spherical morphology and the diameter is around 35 nm, as reported in our previous work [14]. As expected, the modified lignin particles have larger diameter (around 60 nm). The precipitation of *m*-LNP in the inserted image also confirmed the variation of LNP morphology. Meanwhile, the edge became more blurry after the modification. Thus, all the above results highlight the favoring silanization and fluorination modification.

3.2. Hydrophobicity and density of PLA hybrid foams

Fig. 3 exhibited various PLA foam samples and their physical parameters. The density of the PLA foam was approx. 0.085 g/cm^3, highlighting the typical light-weight foam, which were steadily floated on the leaves of the *Scindapsus sureus*. When increasing the *m*-LNP loading, the density decreased slightly to 0.076 g/cm^3. The porosity of the foams is defined as $1-\rho/\rho_0$, where ρ and ρ_0 are the density of the porous architectures and relevant solid PLA, respectively. In other words, the porosity increased from 93.0% to 94.0% when 6 wt% of *m*-LNP was impregnated. Loading *m*-LNP into PLA could reduce the degree of shrinkage and collapsing during freeze-drying, which was probably due to the introduction of the rigid aromatic skeleton of *m*-LNP. It is obvious that with increasing the *m*-LNP content, the hydrophobic of the foam was significantly enhanced, as the water contact angle of PLA-6L sample increased from 124.8° (neat PLA) up to 141°. Actually, the high

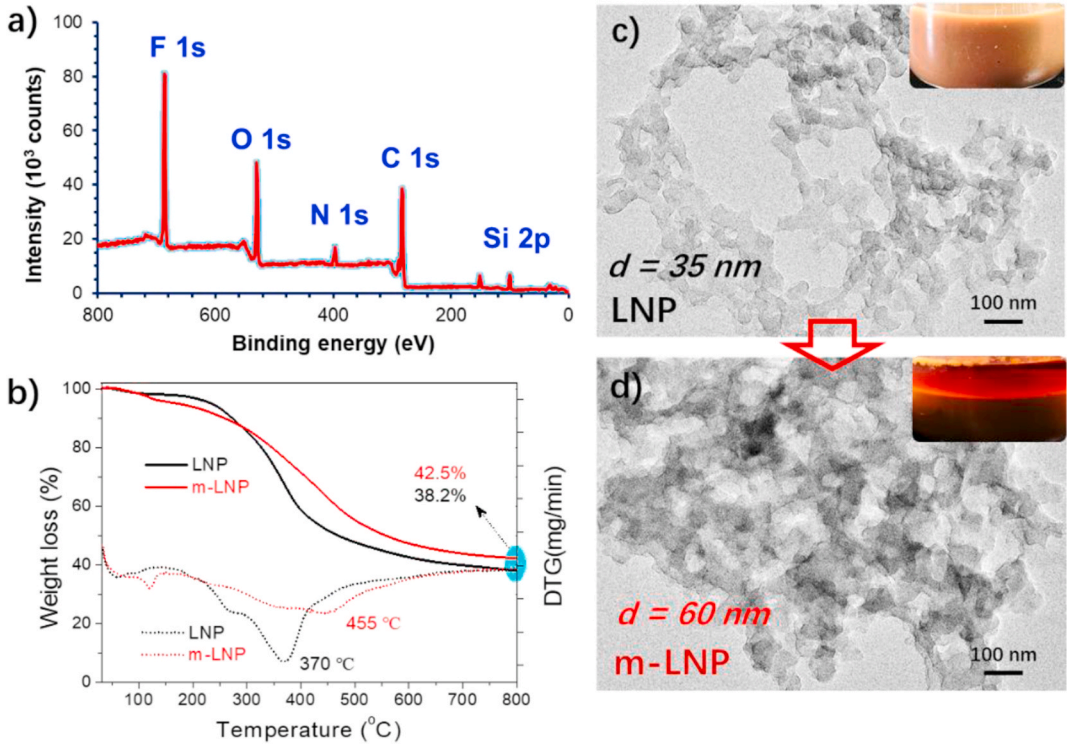

Fig. 2. A) XPS spetrum of *m*-LNP; b) TGA and DTG of LNP and *m*-LNP; c) and d) TEM images of LNP and *m*-LNP.

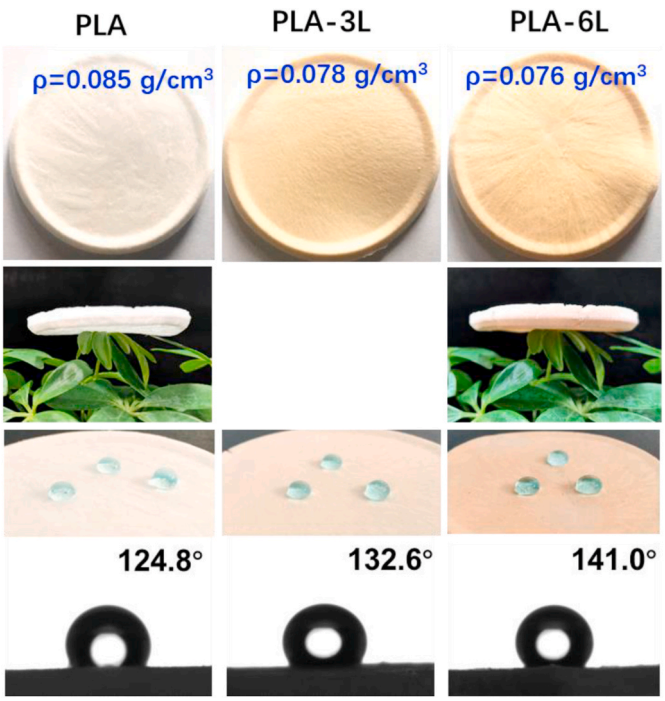

Fig. 3. The density and wettability of PLA hybrid foam samples.

hydrophobic surface could be built after the proper treatment through different fluoroalkyl silane compounds to reduce the wettability [23]. The fluorinated LNP, as the low surface energy molecule, will construct more organized surface structure by minimizing the interaction energy with water during freezing-dry, leading to a highly hydrophobic surface [15]. Meanwhile, as more *m*-LNP was added, the porous walls had more *m*-LNP deposited on them and since *m*-LNP is more hydrophobic than PLA, resulting in a higher hydrophobicity [24]. Generally, the samples with large water contact angle would absorb more oil/organic solvent with higher adsorption rate [16,25]. Actually, in real application, a super hydrophobicity surface is unnecessary for the oil/organic solvents adsorption, and a high hydrophobicity and oleophilicity properties are enough. In other words, the fluorinated foams could collect a wide range of oil/organic solvents with excellent absorption capacities, which exceeded most pure polymer-based foams/aerogels [26]. The thermal stability of the studied foams was also available in Fig. S2, and the addition of *m*-LNP obvious delayed the thermo-decomposition of PLA.

3.3. Morphology of PLA foams

The pore structure is the key to influence the mechanical (free-standing) and absorption properties for the foam samples. To ascertain the pore diameter and its distribution parameter, around 100 pores in the SEM images of each specimen are analyzed by an ImageJ software. The average pore diameter (d_w) and its distribution parameter (σ) were then determined through the following equation:

$$d_w = \frac{\sum_{i=1}^{N} n_i d_i^2}{\sum_{i=1}^{N} n_i d_i} \quad (1)$$

$$ln\ \sigma = \sqrt{\frac{\sum_{i=1}^{N} n_i (lnd_i - lnd_w)^2}{\sum_{i=1}^{N} n_i}} \quad (2)$$

where n_i and d_i represent the pore number and diameter, respectively. σ is set as 1 in case of mono-dispersity in this work [27]. The thickness (t) of foam cell was also calculated. Fig. 4 exhibits the SEM morphology of various PLA foam samples at different scale, and the d_w, σ and t were inserted in the images. It is clear that with increasing the *m*-LNP content to 6 wt%, the d_w and σ decreased from 47 μm to 1.6–32 μm and 1.2, while t declined from 7.6 μm to only the one-third value (2.5 μm), respectively. These results mean that PLA foam impregnating with *m*-LNP have higher porosity than pure PLA, which will contributed to accelerating the oil/organic solvents absorption capacity [24].

3.4. Oil/organic solvent absorption

Fig. 5a demonstrates the absorption rate of various PLA composite foams when absorbing Sudan Red 4/toluene mixture. As expected, with impregnating the *m*-LNP, the absorption rate was accelerated. It needs 10.1s to absorb completely the oil for pure PLA foam, while it only needs 6.1 and 4.8s for PLA-3L and PLA-6L samples. Since *m*-LNP was added, the porous walls had more *m*-LNP deposited on them and a higher hydrophobic structure was constructed, consequently leading to higher rate of oil/organic solvents absorption by the porous structure [24]. In

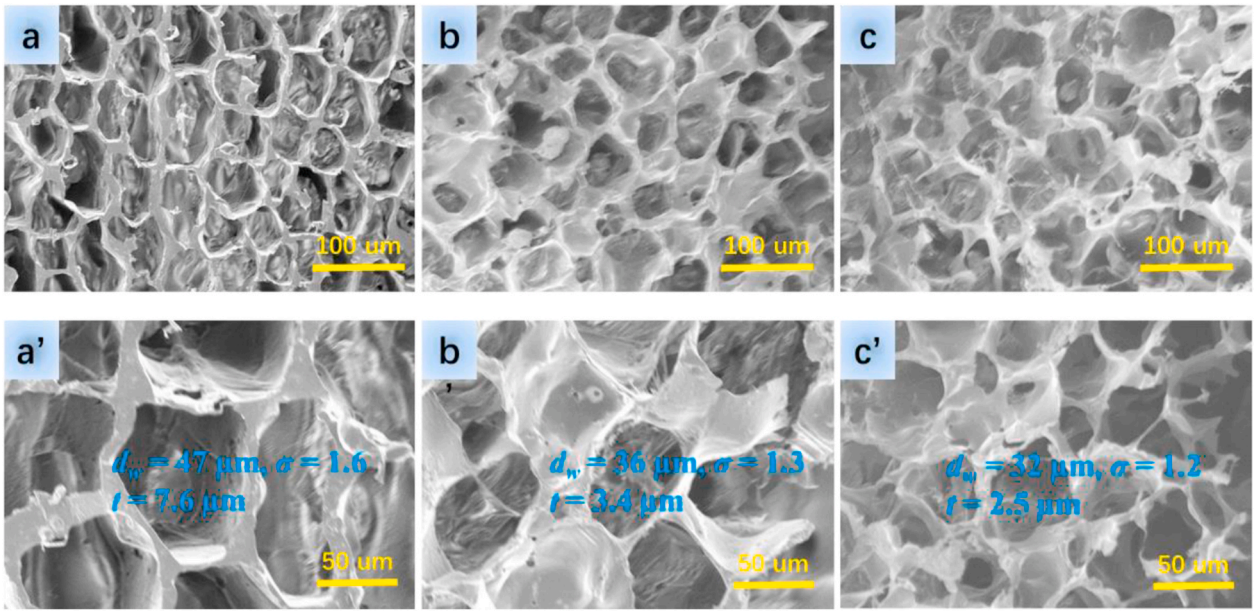

Fig. 4. SEM morphology images of various PLA foam samples (a, a': PLA; b, b': PLA-3L; c, c': PLA-6L).

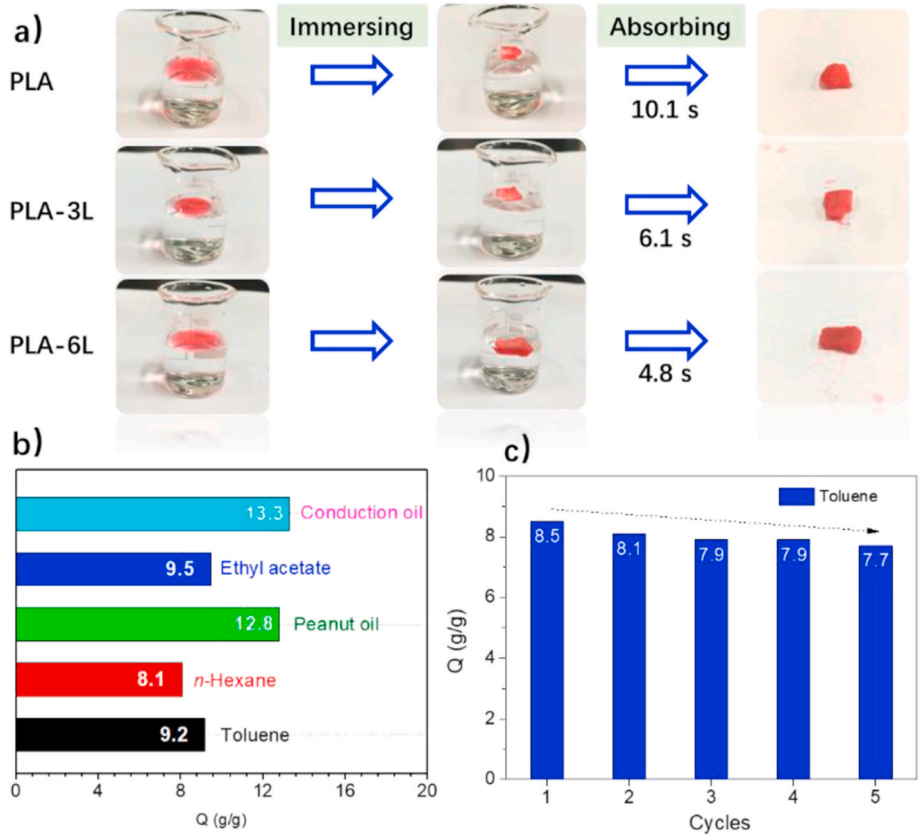

Fig. 5. The absorption rate of Sudan Red 4/toluene mixture for various PLA foams (a); the absorption capacity (b) and cycles (c) of the representative PLA-3L sample. (For interpretation of the references to colour in this figure legend, the reader is referred to the Web version of this article.)

the meanwhile, the lower density and favorable porosity for the composite foams will also contribute the higher absorption rate. This result was in accordance with the above discussion. Due to the small difference in absorption rate between two composite foams, the porous PLA-3L foam sample was utilized in the subsequent absorption experiments.

Fig. 5b and c showed the absorption capacity and cycles of the representative PLA-3L sample, and the absorption cycles for the *n*-hexane and ethyl acetate have been also added in Fig. S3. It is well-known that the absorption capacity relies on the density of the oil/organic solvents [28]. The *Q* values for the various oil/organic solvents after absorbing 10 s are in the order: conductive oil (*Q*: 13.3, density: 1.022 g/cm^3) > peanut oil (12.8, 0.915) > ethyl acetate (9.5, 0.902) > toluene (9.2, 0.866) > *n*-hexane (8.1, 0.66). Thus, this order is in accordance with the density of the oil/organic solvents, and similar results were also reported in other porous absorbents [24,29]. The absorption capacity for all the selective solvents almost reached their respective saturated adsorption capacity at such short time, which was ascribed to two factors: the high hydrophobicity and high porosity, as confirmed above. In other words, the absorption is based on surface structure of the pore cell and the void volume in the porous materials.

Recyclability is an significant assessment criteria for oil/organic solvents absorption in practical application [19]. Herein, the toluene was chosen as the absorbate. After 5 evaporation−adsorption cycles, the PLA-3L foam sample still maintains more than 91.0% of its original capacity, indicating favorable recyclability behavior. The toluene could gently enter and left the foam without destroying the porous structure, which significantly improves its cycling capacity.

4. Conclusions

In this study, the hydrophobic lignin nanoparticles were first synthesized via a synchronous modification of silanization and fluorination process. Then the bio-based PLA foams for oil/organic solvents absorption application were prepared via freezing-dry method by impregnating various amount of *m*-LNP. The impregnation of *m*-LNP improved the thermal stability of PLA foams due to the formation of Si–O–C networks in lignin skeleton, which possesses higher pyrolysis enthalpy than that of C–O bond. Simultaneously, the *m*-LNP also contributed higher hydrophobic surface and high porosity of the resulting composite foams. As a consequent, the composite foam will accelerate the absorption rate and reach the saturated adsorption capacity in quite short time, meanwhile exhibiting good recyclability, which is significant in practical application. This work may pay the way to develop a fully biodegradable absorbent for the oil/organic contaminant.

CRediT authorship contribution statement

Hui Ding: Data curation, Writing – original draft, Funding acquisition, Methodology, Formal analysis. **Weijun Yang:** Data curation, Writing – original draft, Funding acquisition, Methodology, Formal analysis, Conceptualization, Validation. **Wenhao Yu:** Data curation, Writing – original draft, Funding acquisition. **Tianxi Liu:** Resources, Writing – review & editing. **Haigang Wang:** Resources, Writing – review & editing. **Pengwu Xu:** Resources, Writing – review & editing. **Liangliang Lin:** Resources, Writing – review & editing. **Piming Ma:** Data curation, Writing – original draft, Funding acquisition, Conceptualization, Validation, Formal analysis.

Declaration of competing interest

The authors declare that they have no known competing financial interests or personal relationships that could have appeared to influence the work reported in this paper.

Acknowledgements

This work was financially supported by National Science Foundation of China (51903106, 51873082, 52073123), Distinguished Young Natural Science Foundation of Jiangsu Province (BK20200027), the Key Laboratory of Bio-based Material Science & Technology (Northeast Forestry University), Ministry of Education (SWZ-ZD201904).

Appendix A. Supplementary data

Supplementary data to this article can be found online at https://doi.org/10.1016/j.coco.2021.100730.

References

[1] J. Yuan, X. Liu, O. Akbulut, J. Hu, S.L. Suib, J. Kong, et al., Superwetting nanowire membranes for selective absorption, Nat. Nanotechnol. 3 (6) (2008) 332–336.
[2] D.D. Nguyen, N.-H. Tai, S.-B. Lee, W.-S. Kuo, Superhydrophobic and superoleophilic properties of graphene-based sponges fabricated using a facile dip coating method, Energy Environ. Sci. 5 (7) (2012) 7908–7912.
[3] H. Sun, A. Li, Z. Zhu, W. Liang, X. Zhao, P. La, et al., Superhydrophobic activated carbon-coated sponges for separation and absorption, ChemSusChem 6 (6) (2013) 1057–1062.
[4] Q. Wen, J. Di, L. Jiang, J. Yu, R. Xu, Zeolite-coated mesh film for efficient oil–water separation, Chem. Sci. 4 (2) (2013) 591–595.
[5] X. Gui, J. Wei, K. Wang, A. Cao, H. Zhu, Y. Jia, et al., Carbon nanotube sponges, Adv. Mater. 22 (5) (2010) 617–621.
[6] C. Chen, F. Li, Y. Zhang, B. Wang, Y. Fan, X. Wang, et al., Compressive, ultralight and fire-resistant lignin-modified graphene aerogels as recyclable absorbents for oil and organic solvents, Chem. Eng. J. 350 (2018) 173–180.
[7] T. Zhang, L. Kong, Y. Dai, X. Yue, J. Rong, F. Qiu, et al., Enhanced oils and organic solvents absorption by polyurethane foams composites modified with MnO2 nanowires, Chem. Eng. J. 309 (2017) 7–14.
[8] O.S.H. Santos, M. Coelho da Silva, V.R. Silva, W.N. Mussel, M.I. Yoshida, Polyurethane foam impregnated with lignin as a filler for the removal of crude oil from contaminated water, J. Hazard Mater. 324 (2017) 406–413.
[9] B. Doshi, M. Sillanpää, S. Kalliola, A review of bio-based materials for oil spill treatment, Water Res. 135 (2018) 262–277.
[10] J. Feng, S.T. Nguyen, Z. Fan, H.M. Duong, Advanced fabrication and oil absorption properties of super-hydrophobic recycled cellulose aerogels, Chem. Eng. J. 270 (2015) 168–175.
[11] B. Doshi, E. Repo, J.P. Heiskanen, J.A. Sirviö, M. Sillanpää, Effectiveness of N,O-carboxymethyl chitosan on destabilization of Marine Diesel, Diesel and Marine-2T oil for oil spill treatment, Carbohydr. Polym. 167 (2017) 326–336.
[12] Y. Yang, Y. Deng, Z. Tong, C. Wang, Renewable lignin-based xerogels with self-cleaning properties and superhydrophobicity, ACS Sustain. Chem. Eng. 2 (7) (2014) 1729–1733.
[13] Y. Yang, H. Yi, C. Wang, Oil absorbents based on melamine/lignin by a dip adsorbing method, ACS Sustain. Chem. Eng. 3 (12) (2015) 3012–3018.
[14] W. Yang, E. Fortunati, D. Gao, G.M. Balestra, G. Giovanale, X. He, et al., Valorization of acid isolated high yield lignin nanoparticles as innovative antioxidant/antimicrobial organic materials, ACS Sustain. Chem. Eng. 6 (3) (2018) 3502–3514.
[15] A. Baidya, M.A. Ganayee, S. Jakka Ravindran, K.C. Tam, S.K. Das, R.H.A. Ras, et al., Organic solvent-free fabrication of durable and multifunctional superhydrophobic paper from waterborne fluorinated cellulose nanofiber building blocks, ACS Nano 11 (11) (2017) 11091–11099.
[16] X. Wang, Y. Pan, X. Liu, H. Liu, N. Li, C. Liu, et al., Facile fabrication of superhydrophobic and eco-friendly poly(lactic acid) foam for oil–water separation via skin peeling, ACS Appl. Mater. Interfaces 11 (15) (2019) 14362–14367.
[17] X. He, F. Luzi, W. Yang, Z. Xiao, L. Torre, Y. Xie, et al., Citric acid as green modifier for tuned hydrophilicity of surface modified cellulose and lignin nanoparticles, ACS Sustain. Chem. Eng. 6 (8) (2018) 9966–9978.
[18] C.G. Boeriu, D. Bravo, R.J.A. Gosselink, J.E.G. van Dam, Characterisation of structure-dependent functional properties of lignin with infrared spectroscopy, Ind. Crop. Prod. 20 (2) (2004) 205–218.
[19] W. Ma, M. Zhang, Z. Liu, M. Kang, C. Huang, G. Fu, Fabrication of highly durable and robust superhydrophobic-superoleophilic nanofibrous membranes based on a fluorine-free system for efficient oil/water separation, J. Membr. Sci. 570 (2019) 303–313.
[20] S. Iravani, R.S. Varma, Greener synthesis of lignin nanoparticles and their applications, Green Chem. 22 (3) (2020) 612–636.
[21] P. Khanjani, A.W.T. King, G.J. Partl, L.-S. Johansson, M.A. Kostiainen, R.H.A. Ras, Superhydrophobic paper from nanostructured fluorinated cellulose esters, ACS Appl. Mater. Interfaces 10 (13) (2018) 11280–11288.
[22] Y. Lu, Y. Wang, L. Liu, W. Yuan, Environmental-friendly and magnetic/silanized ethyl cellulose sponges as effective and recyclable oil-absorption materials, Carbohydr. Polym. 173 (2017) 422–430.
[23] Y. Zhang, T. Ren, T. Li, J. He, D. Fang, Paper-based hydrophobic/lipophobic surface for sensing applications involving aggressive liquids, Advanced Materials Interfaces 3 (22) (2016) 1600672.
[24] Y. Liu, G. Huang, C. Gao, L. Zhang, M. Chen, X. Xu, et al., Biodegradable polylactic acid porous monoliths as effective oil sorbents, Compos. Sci. Technol. 118 (2015) 9–15.
[25] J.-Y. Hong, E.-H. Sohn, S. Park, H.S. Park, Highly-efficient and recyclable oil absorbing performance of functionalized graphene aerogel, Chem. Eng. J. 269 (2015) 229–235.
[26] J. Wang, W. Zhang, C. Zhang, Versatile fabrication of anisotropic and superhydrophobic aerogels for highly selective oil absorption, Carbon 155 (2019) 16–24.
[27] B. Wu, P. Xu, W. Yang, M. Hoch, W. Dong, M. Chen, et al., Super-toughened heat-resistant poly(lactic acid) alloys by tailoring the phase morphology and the crystallization behaviors, J. Polym. Sci. 58 (3) (2020) 500–509.
[28] H. Bi, X. Xie, K. Yin, Y. Zhou, S. Wan, L. He, et al., Spongy graphene as a highly efficient and recyclable sorbent for oils and organic solvents, Adv. Funct. Mater. 22 (21) (2012) 4421–4425.
[29] H.W. Liang, Q.F. Guan, L.F. Chen, Z. Zhu, W.J. Zhang, S.H. Yu, Macroscopic-scale template synthesis of robust carbonaceous nanofiber hydrogels and aerogels and their applications, Angew. Chem. Int. Ed. 51 (21) (2012) 5101–5105.